Vibrational Spectroscopic Properties of Hydrogen Bonded Acetonitrile Studied by DFT

Jose M. Alía*,† and Howell G. M. Edwards**

Departamento de Química-Física, E.U.I.T.A., Universidad de Castilla-La Mancha, Ronda de Calatrava 7, 13071 Ciudad Real, Spain, and Chemical and Forensic Sciences, School of Pharmacy, University of Bradford, Bradford, BD7 1DP, U.K.

Received: April 12, 2005

Vibrational properties (band position, Infrared and Raman intensities) of the acetonitrile C≡N stretching mode were studied in 27 gas-phase medium intensity (length range: = 1.71−2.05 Å; $-\Delta E$ range = 13−48 kJ/mol) hydrogen-bonded 1:1 complexes of CH_3CN with organic and inorganic acids using density functional theory (DFT) calculations [B3LYP-6-31++G(2d,2p)]. Furthermore, general characteristics of the hydrogen bonds and vibrational changes in the OH stretching band of the acids were also considered. Experimentally observed blue-shifts of the C≡N stretching band promoted by the hydrogen bonding, which shortens the triple bond length, are very well reproduced and quantitatively depend on the hydrogen bond length. Both predicted enhancement of the infrared and Raman ν(C≡N) band intensities are in good agreement with the experimental results. Infrared band intensity increase is a direct function of the hydrogen bond energy. However, the predicted increase in the Raman band intensity increase is a more complex function, depending simultaneously on the characteristics of both the hydrogen bond (C≡N bond length) and the H-donating acid polarizability. Accounting for these two parameters, the calculated ν(C≡N) Raman intensities of the complexes are explained with a mean error of ±2.4%.

1. Introduction

The important modifications promoted in the vibrational dynamics of the nitrile functional group under the effect of chemical coordination with Lewis acids involving the nitrogen lone pair are firmly documented both theoretically[1−6] as well as from the experimental point of view (for two reviews on the infrared (IR) and Raman spectroscopic aspects, see refs 7 and 8, respectively). The first attempt to computationally approach the changes in the structural and vibrational characteristics of the acetonitrile C≡N bond under the effect of coordination was undertaken by Vijay and Sathayanarayana,[9] who studied the complexes formed between borane and acetonitrile/methyl isocyanide both experimentally and from ab initio calculations using HF/DZP and MP2/DZP methods. A shortening of both the N≡C (isocyanide) and C≡N (acetonitrile) bonds as a result of complexation with the boron atom were predicted by theoretical calculations and observed experimentally. The immediate effect of this change was to strengthen the corresponding bond force constants, thus increasing significantly the C≡N/N≡C stretching frequencies (+100 cm^{-1} in acetonitrile and +150 cm^{-1} in methyl isocyanide). Experimental infrared intensities were greatly enhanced as predicted by these ab initio calculations at both levels of theory.

A special and interesting case of acetonitrile coordination is the hydrogen bond (HB) formation through the nitrogen lone pair. Coussan et al.[10] studied by IR spectroscopy the complex $CH_3OH\cdots NCCH_3$ in Ar or N_2 matrices, including a detailed computational calculation using DFT at the B3LYP/6-31(and 6-311)++G(2d,2p)) levels. The calculated dissociation energy of the complex was 18.13 kJ/mol (BSSE corrected) with an HB distance of 2.07 Å and a predicted shift of 12.6 cm^{-1} in the corresponding C≡N stretching band (experimentally observed: 9.3 cm^{-1}). Galabov and Bobadova-Parvanova[11] carried out a systematic study at the HF/6-31+(d,p) level of the geometry and energy of 1:1 hydrogen-bonded complexes between hydrogen fluoride and a series of 11 nitriles. The range of dissociation energies (BSSE corrected) was 7.8−26.5 kJ/mol, with a value of 24.4 kJ/mol for acetonitrile. The corresponding N···H distance was 1.9372 Å. George et al.[12] obtained almost linear geometries for 1:1 hydrogen-bonded complexes between five nitriles (including HCN) and hydrogen chloride at the B3LYP/6-311++G(2d,2p) level of theory. The complex $CH_3CN\cdots HCl$ shows an HB length of 1.9792 Å with a predicted 16.6 kJ/mol of dissociation energy. In this paper, the reported C≡N stretching shifts fluctuate between 14.1 and 17.4 cm^{-1} depending on the nitrile, with a value of 15.5 cm^{-1} for acetonitrile. The authors conclude that DFT is a suitable tool to assess the geometries, energy, and vibrational characteristics of such complexes. Kryachko and Nguyen[13] studied several complexes between phenol and acetonitrile, comparing the MP2 and DFT approaches. The σ-bonded complex is a slightly bent structure ($\angle$(C≡N···H) = 169.1°), with N···H distances of 1.997 (DFT) and 2.034 Å (MP2) and dissociation energies (BSSE corrected) of 22.4 (DFT) and 29.5 (MP2) kJ/mol. The C≡N stretch blue shift is evaluated as 14−15 (DFT) and 16 cm^{-1} (MP2). However, no data on the vibrational intensities are available. Rissi et al.[14] have studied the complex $CH_3CN\cdots H_2O$ using four different theory levels, namely MP2/6-311++G(d,p), MP2/aug-cc-pVDZ, B3LYP/6-311++G(d,p), and B3P86/6-311++G(d,p). Depending on the theory level adopted, the N···H distances are located in the range 2.036−2.106 Å, with MP2 lengths longer than those predicted on the basis of the DFT calculations. BSSE-corrected dissociation energies are in the range 13.5−17.7 kJ/mol, with a best value

* Corresponding author. E-mail: josemaria.alia@uclm.es.
† Universidad de Castilla-La Mancha.
‡ University of Bradford.

10.1021/jp051892y CCC: $30.25
Published on Web 08/12/2005

TABLE 1: Molecular Parameters of Acetonitrile at Different Levels of Theory and Basis Sets Where Experimental Data Are from References 29 and 39

level of theory	basis set	C−C (Å)	C−H (Å)	C≡N (Å)	∠(CH) (deg)	ϵ (D)	α (Å^3)	mean error (%)
HF	6-31++(d,p)	1.467	1.082	1.136	109.7	4.229	3.66	8.73
	6-31++(2d,2p)	1.467	1.081	1.132	109.7	4.250	3.83	8.37
	6-311++(d,p)	1.465	1.082	1.130	109.7	4.203	3.70	8.53
	6-311++(2d,2p)	1.465	1.079	1.127	109.7	4.229	3.87	8.34
MP2	6-31++(d,p)	1.463	1.088	1.181	109.9	4.328	3.82	5.39
	6-31++(2d,2p)	1.464	1.088	1.176	110.0	4.349	4.01	3.91
	6-311++(d,p)	1.457	1.095	1.164	110.4	4.274	3.88	3.94
	6-311++(2d,2p)	1.461	1.085	1.169	110.0	4.322	4.05	3.80
DFT	6-31++(d,p)	1.461	1.094	1.161	110.2	4.077	4.00	2.83
	6-31++(2d,2p)	1.460	1.092	1.157	110.2	4.088	4.16	2.53
	6-311++(d,p)	1.456	1.092	1.153	110.2	4.054	4.01	2.81
	6-311++(2d,2p)	1.457	1.089	1.150	110.2	4.065	4.18	2.59
	Exptl	***1.468***	***1.107***	***1.159***	***109.7***	***3.924***	***4.44***	

of 14.8 kJ/mol. The MP2 calculated C≡N stretching shifts are greater than those corresponding to the DFT calculations (17 vs 10 cm^{-1}, respectively). Raman band intensities are calculated only at the MP2/aug-cc-pVDZ level of theory and a moderate increase of the C≡N stretching band depolarization ratio (from 0.17 up to 0.20) is reported upon HB formation. Consequently, its Raman intensity rises from 49.37 Å^4/amu in acetonitrile to 64.02 Å^4/amu in the complex. Recently, Chaban[15] has studied 1:1 complexes between water and three different nitriles (namely, $H_2N-C\equiv N$, $CH_3-C\equiv N$, and $H_2N-CH_2-C\equiv N$) at the MP2/TZP level in distinct configurations. When the C≡N group acts as the σ-acceptor, predicted dissociation energies (BSSE uncorrected) are in the range 15.4−17.2 kJ/mol, with a value of 15.7 kJ/mol for acetonitrile. Calculated anharmonic C≡N stretching blue-shifts are significant (19−23 cm^{-1}) and the IR intensities, which are the only ones reported, increase from 1.36 up to 2.29 times after HB formation. Thus, although the experimental facts, i.e., blue-shift of the C≡N stretching band, strong increase of the infrared (IR) absorption coefficient, and moderate to medium increase of the corresponding Raman intensity, are clearly predicted (see refs 16−21 for further discussion), a complete explanation of these findings and their dependence to the best of our knowledge is lacking in the literature.

In this paper, we present a detailed study of the optimized structures and vibrational spectra, including the Raman intensities, of 27 H-bonded 1:1 acetonitrile complexes with organic and inorganic acids (see Table 4 for a complete list) with the aim to understand the factors which influence the modulation of the changes in the C≡N stretching dynamics that have been reported above. Despite initial criticisms,[22] density functional theory has been successfully employed to assess the geometries, energies, and vibrational spectra of H-bonded complexes,[12,23−27] and recently[28] its accuracy and good agreement with MP2 and coupled-cluster methods has been confirmed for H-bonds that do not deviate significantly from linearity. Thus, taking into account the computational time spent for moderately big atomic systems (on average, complexes studied in this paper need 218 basis functions and 324 primitive Gaussians) for which Raman intensities are also required, we have decided to employ in this paper DFT with a medium-complexity basis including both diffuse and polarization functions that secures the quality of results needed in a systematic study where the main interest is the assessment of general trends instead of evaluating one specific system with a very high precision.

2. Computational Details

Starting structures for the single compounds, when available in the gas phase, were taken from the literature.[29,30] In those cases where such information was not available, structures were initially optimized by a semiempirical method (PM3) and, then, refined using DFT calculations. Becke's gradient corrected exchange functional[31] in conjunction with the Lee−Yang−Parr correlation functional[32] with three parameters (B3LYP)[33] was used throughout. All the final DFT-optimized structures possessed a minimum of the PES as can be inferred from the absence of negative (imaginary) frequencies. These structures and their corresponding vibrational spectra are available on demand. Once optimized, the structure and its electrostatic properties including the electrostatic potential at atomic sites were obtained. Optimized structures of both the acid and the base (acetonitrile) were located initially at an N···H distance of 2 Å with the C, N, O, and H atoms in the same line as initial parameters up to the convergence of the structure. In a second run, the same molecules were located initially at the same distance, but forming a C−N−H angle of 135°. The converged structure was accepted only if does not differ from that previously optimized with the linear configuration as a starting point and was free of imaginary frequencies. The structures and spectra of the complexes are available on demand. The zero-point vibrational energies calculated within the harmonic approximation and the thermal energies and enthalpies at 298 K were calculated using the unscaled harmonic vibrational frequencies. The effect of the basis-set superposition error (BSSE) was analyzed in the optimized structure of the complexes by the standard counterpoise method.[34,35] Usually, the complex binding energy is defined as

$$\Delta E = [E_{\text{complex}} - (E_{\text{acid}} + E_{\text{CH3CN}})] + E_{\text{BSSE}}$$

where

$$E_i = E_{\text{electronic}} + E_{\text{ZPE}} \quad (i = \text{acid, } CH_3CN \text{ or complex})$$

All these calculations were carried out with the Gaussian03 program package[36] in the Supercomputation Centre of the Universidad de Castilla-La Mancha, which uses the machines HP AlphaServer GS80 and Silicon Graphics Origin 2000. The Ampac Gui 8 system[37] was the graphic interface that, in particular, allows to study conveniently the vibrational modes. Statistical (curve-fitting) procedures were run with the application STATGRAPHICS+ (5.1) for Windows.[38]

3. Results and Discussion

3.1. Evaluation of the Level of Theory and Basis Set. To evaluate the confidence of the level of theory and basis set that are used in this work [B3LYP/6-31++G(2d,2p)], we undertook a series of calculations to compare the geometry and vibrational

spectroscopic results obtained for acetonitrile at three levels of theory (Hartree−Fock, Møller−Plesset, and DFT with the B3 functional and the nonlocal correlation of Lee, Yang, and Parr) and four different standard basis sets, namely 6-31++G(d,p), 6-31++G(2d,2p), 6-311++G(d,p), and 6-311++G(2d,2p). With the same initial parameters (those corresponding to the experimental structure in the gas phase[29]), geometric parameters and two molecular properties (dipole moment and mean polarizability) were estimated in the optimized structures. The results are shown in Table 1. As can be observed, DFT gives the best results with mean errors significantly lower than the corresponding HF or MP2 levels. This is particularly evident in the C≡N bond length, which is an important parameter in the present work, that seems to be overestimated in the MP2 level in agreement with previous results.[13,14] In the DFT level calculations the 6-311 basis sets tend to short the bond distances, as previously reported,[10] when compared with the 6-31 basis set.

Table 2 shows the vibrational wavenumbers corresponding with the optimized structures. Experimental data[39] are from the gaseous state which slightly differ from the data obtained from Ar or N_2 matrixes.[10] Here, results from the MP2 and DFT levels are clearly comparable and, if we consider the wavenumber corresponding to the C≡N stretching, more favorable than the MP2 calculation. However, the mean errors are smaller in the DFT level because of its better agreement between the observed and calculated values for the remaining vibrational frequencies, mainly those arising from the CH stretches. As the main interest of the present work is to study the vibrational shifts and not the vibrational frequencies themselves and previous results confirm that these shifts are quite independent of the level of the theory,[11,13,14] data from Table 2 confirm that DFT can provide reliable results.

Vibrational frequencies calculated for the acids have been also checked against the available experimental results.[40−43] Table 3 gives some selected results for acids with a different number of atoms ($n = 3-8$). It can be seen that the general agreement between calculated and experimental data is satisfactory. Data from all the available spectra in the gaseous phase (16 compounds, 142 frequencies) are plotted in Figure 1, which shows the experimental against calculated wavenumber values. From these data, a scaling factor of 0.9623 is obtained at the B3LYP/6-31++G(2d,2p) level. This factor is very close to those recently published[44] for the B3LYP density functional method with the triple-ζ basis set 6-311+G(d,p). However, in this work we will not apply any scale correction factor for the frequencies nor in the ZPE correction.

3.2. General Characteristics of the Hydrogen Bonds. Table 4 shows the geometrical and energetic parameters of the H-bonded complexes studied here. As can be observed, all the HB can be classified as moderate on the basis of the energetic and geometrical parameters.[45−47] One interesting feature of the results is the almost linear geometry of the calculated HB: except for CH_3SO_3H and HCOOH, all the C≡N···H angles are ≥165°. This finding contrasts with the situation found in the solid state. In a review[46] of over 95 cases of R−OH hydrogen bonds to nitrile nitrogen, the average C≡N···H angle was 145±23°. If we consider that the complementary angle, i.e., the ∠(O−H···N), is even, closer to 180°, it must be concluded that the C≡N···H−O interactions are prone to the adoption of a linear geometry, which in turn supports the suitable use of the DFT method for their study.[28]

The relationship between the HB length and the energy parameters has been thoroughly investigated[45,47−51] over many years. Sokolov[50] proposed an electrostatic model of the HB, mainly developed to understand the vibrational OH shifts when water molecules coordinate with a cation, from which the energy of the HB was proposed to be an exponential function of the HB distance, namely:

$$|\Delta E| = -Z_H|Z_B|\left(\frac{1}{R_{HB}} - \frac{1}{R_{AB}}\right) + Ce^{-\beta R^{HB}}$$

where C and β are constants that depend on the characteristics of the potential well (C) and the O−H bond (β), B represents the base, R_{HB} is the HB length and R_{AB} the bond distance of the acid A−H. The first term of the sum is very small because distances are in Å and charges are fractional (Mulliken charges). So, a direct exponential function of ΔE against d(N···H) should be expected.

TABLE 2: Calculated Harmonic Vibrational Frequencies (cm^{-1}) of Acetonitrile at Different Levels of Theory and Basis Sets (A, 6-31++G(d,p); B, 6-31++(2d,2p); C, 6-311++(d,p); D, 6-311++(2d,2p)), Where Experimental Data Are from Reference 40

		HF			
normal mode	exptl	A	B	C	D
CCN bending	362	421.8	423.3	424.6	422.5
CCN bending	362	421.9	423.3	424.6	422.5
CC stretch	920	967.5	961.1	964.6	957.5
CH_3 rocking	1041	1161.1	1156.1	1157.9	1161.4
CH_3 rocking	1041	1161.1	1156.2	1157.9	1161.5
CH_3 *s* bending	1385	1540.8	1533.3	1531.1	1538.8
CH_3 *as* bending	1448	1596.9	1595.2	1593.3	1599.3
CH_3 *as* bending	1448	1597.0	1595.2	1593.3	1599.3
CN stretch	2267	2605.4	2594.4	2594.2	2583.2
CH *s* stretch	2954	3218.5	3205.0	3202.5	3209.0
CH *as* stretch	3009	3302.8	3288.4	3281.0	3282.9
CH *as* stretch	3009	3302.9	3288.4	3281.0	3282.9
mean error (%)		***11.378***	***11.082***	***11.119***	***11.117***
		MP2			
normal mode	exptl	A	B	C	D
		334.6	360.3	355.1	362.5
		334.6	360.3	355.1	362.5
		939.2	927.8	933.7	923.7
		1081.4	1073.1	1069.8	1078.2
		1081.4	1073.1	1069.8	1078.2
		1455.2	1433.4	1424.7	1438.7
		1520.9	1507.1	1499.6	1508.5
		1520.9	1507.1	1499.6	1508.5
		2217.3	2206.2	2209.7	2198.5
		3142.1	3105.1	3099.6	3106.9
		3243.8	3201.7	3193.8	3196.3
		3243.8	3201.8	3193.8	3196.3
mean error (%)		***5.358***	***3.352***	***3.382***	***3.390***
		DFT			
normal mode	exptl	A	B	C	D
		378.0	380.1	381.8	378.5
		378.1	380.2	381.9	378.6
		930.0	929.4	930.1	923.2
		1059.9	1054.0	1061.2	1063.7
		1059.9	1054.1	1061.3	1063.8
		1415.2	1407.9	1411.9	1418.2
		1478.1	1473.5	1475.0	1480.8
		1478.1	1473.5	1475.0	1480.9
		2365.1	2360.2	2362.6	2353.0
		3058.9	3054.7	3046.7	3056.9
		3136.0	3130.4	3116.4	3123.2
		3136.1	3130.5	3116.5	3123.3
mean error (%)		***3.022***	***2.861***	***3.012***	***2.972***

TABLE 3: Experimental and B3LYP/6-31++G(2d,2p) Calculated Harmonic Vibrational Frequencies (cm^{-1}) and Their Assignments in Some Selected Acids of Three to Eight Atoms[a]

acid	description	exptl	calcd	acid	description	exptl	calcd
HClO[b]	OH stretch	3609.48	3781.48	BO_3H_3[b]	OH stretch	3706	3873
	HOCl bending	1238.62	1256.87		OH stretch	3705	3873
	OCl stretch	724.36	716.70		BO *as* stretch	1429	1452
HBO_2[b]	OH stretch	3681	3879		HOB deform.	1017	1037
	OBO *as* stretch	2023	2081		BOH deform.	1020	1029
	HOB deform.	904	955		BO *s* stretch	866	876
	OBO deform.	516	511	CF_3COOH[c,d]	OH stretch	3587	3753
	HOB deform.	447	458		C═O stretch	1826	1860
HNO_3[b]	OH stretch	3550.00	3731.04		COH bending	1465	1411
	NO_2 *as* stretch	1709.57	1756.03		CF *as* stretch	1300	1246
	mixed	1325.74	1352.61		δ(OH) IP	1244	1184
	mixed	1303.52	1330.84		CF *as* stretch	1182	1140
	ON stretch	879.11	904.28		C−O stretch	1130	1137
	$\delta(ONO_2)$ OP	763.15	780.01		δ(OCO) OP	904	786
	NO_2 scissors	646.83	651.92		CC stretch	825	785
	NO_2 rock	580.30	587.42		OCO bending	708	664
	torsion	458.23	486.30		δ(OH) OP	904	598
CH_3OH[b]	OH stretch	3681	3848		CF_3 *as* deform.	598	597
	CH_3 *as* stretch	3000	3123		CF_3 *as* deform.	515	500
	CH_3 *s* stretch	2844	2998		CCO deform.	419	419
	CH_3 *as* deform	1477	1507		CF_3 *s* deform.	401	386
	CH_3 *s* deform	1455	1477		CF_3 rock	260	260
	OH bending	1345	1371				
	CH_3 rock	1060	1076				
	CO stretch	1033	1042				
	CH_3 *as* stretch	2960	3051				
	CH_3 *as* deform	1477	1495				
	CH_3 rock	1165	1169				
	torsion	295	298				

[a] Key: *as* = asymmetric; *s* = symmetric; OP = out of plane; IP = in plane. [b] Reference 40. [c] Reference 41. [d] Reference 42.

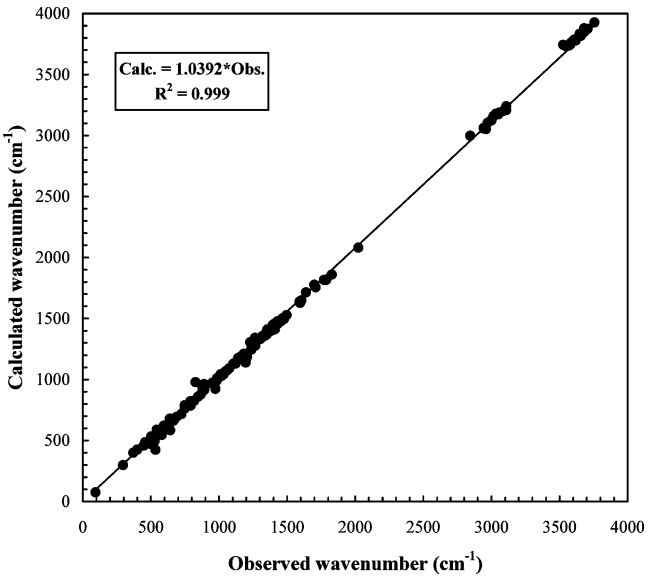

Figure 1. Gas-phase experimental andB3LYP/6-31++G(2d,2p) calculated vibrational frequencies.

Figure 2 plots the absolute values of the BSSE corrected ΔE values against N···H distances (d). Indeed, data can be fitted to an exponential function, with the following characteristics:

$$|\Delta E| = 32\,533 \pm 1.3e^{-3.838\pm0.130d}$$

$$r = -0.9860, \quad R^2 = 97.22\%, \quad N = 27,$$
$$\text{standard error of the estimate} = 0.0621$$

In the limit of the corresponding (N + H) van der Waals radii[52] (2.75 Å), where HB should vanish, $|\Delta H|$ takes a value of 0.85 kJ/mol. For systems of the type $L^{n+}\cdots H_2O$, Sokolov[50] estimates a β parameter of 3.5 $Å^{-1}$ which compares fairly well with that obtained here.

Recently, Galabov et al.[11,53−56] have proposed the use of the electrostatic potential at atomic sites, in particular at the H site (V_H), as a convenient reactivity index in the hydrogen bond formation. The electrostatic potential at one atomic site Y, described first by Kollman[57] and Politzer,[58] is a function of the charges of the remaining atoms, the distances between these atoms and the Y atom and the electronic density of the molecule. This potential, which furthermore is a standard option in Gaussian 03,[36] represents an intrinsic parameter of the acid and, thus, could be used as a predictor of its acidity. Table 5 gives the electrostatic potential at the H site (EPH) in the acids studied here and the corresponding Mulliken charges. These parameters are obtained for the optimized structure of the acids. There is no significant correlation ($r = 0.5048$) between acid H Mulliken charges and the energy of the HB, in good agreement with the previous published results.[55] Figure 3 plots the values of BSSE corrected ΔE against the electrostatic potential of the acid at the H site (V_H). As in previous reports,[11,53−56] there is a satisfactory linear correlation between these parameters that follows the equation

$$\Delta E = -292.74 \pm 12.34 - (281.26 \pm 13.10)V_H$$

$$r = -0.9739, \quad R^2 = 94.85\%, \quad N = 27,$$
$$\text{standard error of the estimate} = 2.1557$$

Although the values of the slope and the intercept depend on the particular proton acceptor and the only data available are for NH_3,[53−55] our results indicate that, for the same acid V_H, ΔE should be smaller in CH_3CN than in NH_3, which agrees with its lower proton affinity (−846.4 kJ/mol in NH_3 against −782 kJ/mol in CH_3CN).[59]

TABLE 4: Energetic and Geometrical Characteristics of the Studied Hydrogen Bonds Calculated at the B3LYP/6-31++(2d,2p) Level of Theory[a]

acid	ΔE (kJ/mol)	ΔE_T (kJ/mol)	ΔH (kJ/mol)	BSSE (kJ/mol)	d(N···H) (Å)	∠(CN···H) (deg)	∠(OH···N) (deg)	d(O···N) (Å)
BO_2H	−41.19	−38.35	−40.83	1.97	1.7736	178.21	179.96	2.7594
BO_3H_3	−18.65	−13.74	−16.22	1.60	1.9410	170.65	176.27	2.9125
CF_3COOH	−37.35	−32.53	−35.01	2.03	1.7892	169.45	175.56	2.7796
CF_3OH	−36.47	−32.31	−34.79	2.04	1.8073	176.44	177.41	2.7929
CF_3SO_3H	−45.17	−41.09	−43.57	2.61	1.7093	171.47	176.62	2.7107
CH_2NOH	−19.73	−15.20	−17.68	1.65	1.9271	172.98	177.73	2.9017
CH_3COOH	−21.96	−17.04	−19.52	1.37	1.9270	166.53	171.06	2.8958
CH_3OH	−15.34	−10.90	−13.38	1.40	2.0478	170.88	178.50	3.0158
CH_3SO_3H	−32.05	−28.06	−30.54	2.19	1.7970	162.51	176.51	2.7862
C_6H_5OH	−19.80	−16.53	−19.01	1.93	1.9689	170.97	170.95	2.9337
ClCOOH	−37.21	−32.55	−35.03	2.07	1.7807	169.01	176.54	2.7732
ClOH	−26.72	−23.44	−25.92	1.74	1.8686	177.66	178.65	2.8514
ClO_2H	−31.93	−27.77	−30.25	1.97	1.8425	166.90	175.43	2.8284
ClO_3H	−28.95	−25.60	−28.07	2.01	1.8488	170.73	178.37	2.8394
ClO_4H	−42.17	−38.55	−41.03	2.50	1.7429	172.71	178.56	2.7447
CNOH	−47.85	−45.16	−47.63	2.21	1.7189	174.55	178.44	2.7157
CO_3H_2	−29.34	−24.73	−27.21	1.80	1.8391	165.00	175.99	2.8140
FCOOH	−38.46	−34.01	−36.49	2.00	1.7792	167.97	177.51	2.7693
FOH	−29.26	−26.13	−28.61	1.68	1.8553	176.99	176.90	2.8407
H_2O	−13.10	−10.79	−13.27	1.26	2.0476	173.17	180.00	3.0177
H_2O_2	−19.59	−15.76	−18.23	1.49	1.9463	173.50	178.13	2.9233
HCOOH	−26.05	−21.80	−24.28	1.57	1.8646	159.58	176.58	2.8501
NH_2OH	−16.32	−13.90	−16.38	1.45	1.9965	173.96	177.07	2.9667
NO_2H	−27.98	−23.79	−26.27	1.80	1.8767	177.08	177.91	2.8611
NO_3H	−35.31	−31.00	−33.48	2.11	1.7947	172.21	170.28	2.7803
SO_3H_2	−27.00	−23.03	−25.50	2.04	1.8580	171.38	175.00	2.8449
SO_4H_2	−39.31	−35.16	−37.64	2.34	1.7501	165.86	178.68	2.7462
mean	***−30.07***	***−26.03***	***−28.51***	***1.88***	***1.8555***	***171.05***	***176.69***	***2.8391***
std dev	***9.50***	***9.64***	***9.64***	***0.34***	***0.0939***	***4.63***	***2.48***	***0.0846***

[a] E_T are the energies obtained after the thermochemistry analysis ($E_T = E + E_{vib} + E_{rot} + E_{trans}$).

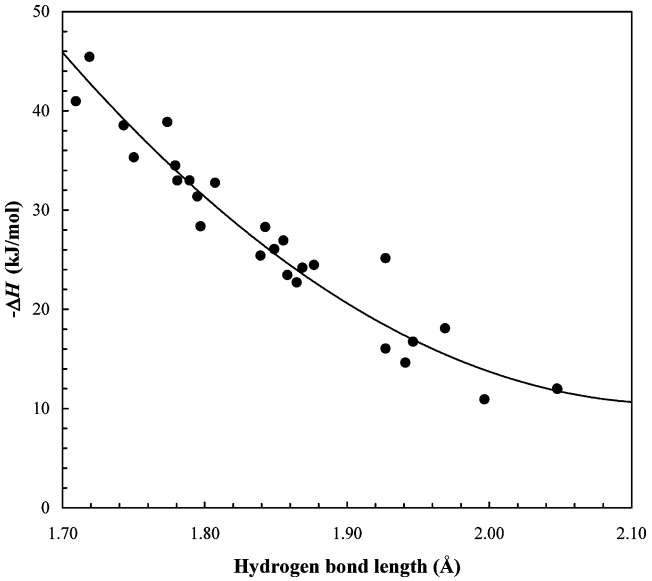

Figure 2. Absolute values of BSSE corrected ΔE against N···H distances in the studied complexes.

TABLE 5: Electrostatic Potential at H Site (au) of the Studied Acids and H Mulliken Charges in Acids at the B3LYP/6-31++(2d,2p) Level of Theory

acid	H site E.P.	H Mulliken q
BO_2H	−0.9044	0.2649
BO_3H_3	−0.9771	0.2396
CF_3COOH	−0.9138	0.2485
CF_3OH	−0.9217	0.2301
CF_3SO_3H	−0.8984	0.2656
CH_2NOH	−0.9805	0.2410
CH_3COOH	−0.9514	0.2154
CH_3OH	−1.0054	0.2147
CH_3SO_3H	−0.9305	0.2654
C_6H_5OH	−0.9727	0.2143
ClCOOH	−0.9178	0.2488
ClOH	−0.9510	0.2463
ClO_2H	−0.9417	0.2426
ClO_3H	−0.9366	0.2509
ClO_4H	−0.9067	0.2487
CNOH	−0.8895	0.2708
CO_3H_2	−0.9381	0.2570
FCOOH	−0.9141	0.2686
FOH	−0.9386	0.2469
H_2O	−0.9955	0.2166
H_2O_2	−0.9769	0.2327
HCOOH	−0.9417	0.2437
NH_2OH	−1.0010	0.2377
NO_2H	−0.9474	0.2301
NO_3H	−0.9154	0.2482
SO_3H_2	−0.9393	0.2390
SO_4H_2	−0.9137	0.2528

3.3. Vibrational Changes in the C≡N Stretch. Table 6 lists the changes promoted in the C≡N bond and its corresponding stretching vibration upon the effect of HB formation. The first point of interest is the general shortening of C≡N bond length, in good qualitative agreement with the experimental results.[46] This shortening, not yet fully understood in theoretical terms,[5,9] has been attributed to conjugative interactions and resonance effects of the nitrile group.[46] The qualitative effect of HB formation upon the distribution of the Mulliken charges in the C≡N bond is the same for all the complexes studied here: there is a drastic reduction (up to 90% in the CF_3SO_3H···$NCCH_3$ complex) of the Δq, expressed as the difference between the C charge (always +) and the N charge (always −), just opposite to that observed in the O−H bond, where the participation of the H atom in HB increases Δq (i.e., *"ionizes"* the bond) and lengthens the O−H distance. Thus, the coordination of the nitrile group through its lone pair should increase the covalency of

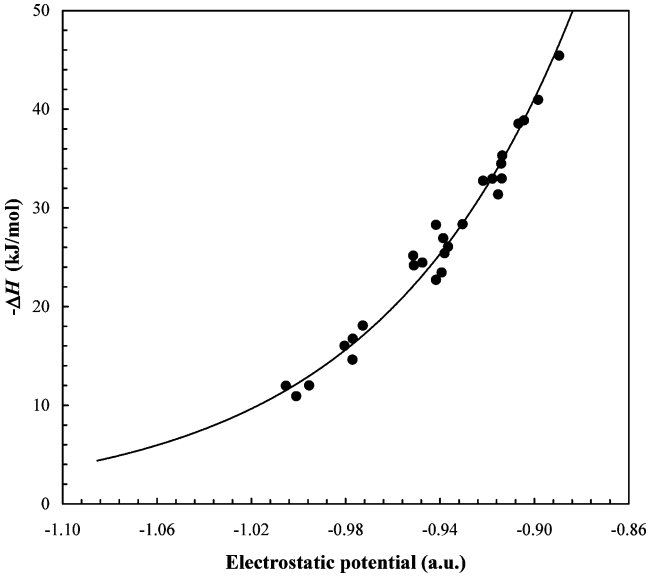

Figure 3. Absolute values of BSSE corrected ΔE against the electrostatic potential of the acid at the H site (V_H).

the C≡N bond. Furthermore, this change can be correlated with the intensity (energy) of the HB. It must be noted that the situation in other multiple bonds (e.g., C═O or C═S) is totally different and resembles the behavior of the O−H bonds. There is enough theoretical and experimental evidence (see refs 60−62 for the most recent studies) which demonstrates that the effects of HB on the C═O bonds are (1) a lengthening of the C═O distance and (2) a decrease of the stretching frequency. The same applies for the C═S double bond.[63,64] Again, charge distributions over the carbonyl bond demonstrate that a Δq increase can result from HB formation, i.e., the bond tends to behave less covalently. Thus, the situation of the C≡N bond is rather characteristic and could be understood in the conceptual frame of the so-called "*improper*" (or blue-shifting) hydrogen bonds.[65] Nitrogen atom transfers electron density to the acceptor (H atom), thus decreasing its original highly negative charge. However, this fact is not compensated by the nitrile C atom which, in turn, increases its own electron density from both the triple bond and the rest of the molecule (H bond in the case of HCN, methyl group in acetonitrile), giving rise to a final situation where the dipolar character of the nitrile group almost disappears, thus increasing its covalency. However, as the situation should be explained in quantitative terms, a natural bond order analysis was undertaken using the NBO 3.1 program[66−68] from a Gaussian03[36] package applied to the optimized structures of CH_3CN, the acids, and the H-bound complexes. Table 7 gives the relevant results concerning the C≡N bond, As can be observed, the main consequences of the HB formation can be summarized as follows: (1) There is an important depletion in the electronic population of the N lone pair which accounts for almost (average: $94.2 \pm 2.3\%$) all the net charge transfer from the base (CH_3CN) to the acid. (2) There is a relative decrease in the total ($\sigma + \pi' + \pi''$) antibonding population calculated as

$$\Delta\rho = (\rho - \rho^*)_{\text{complex}} - (\rho - \rho^*)_{CH_3CN}$$

where ρ and ρ^* are the electronic populations of the bonding and antibonding components of C≡N group. (3) There is a significant increase in the *s* character of the triple bond, mostly promoted by the changes observed in the N center. These three circumstances contribute to the strengthening of the C≡N bond[67−69] and are consequences of the $n \rightarrow \sigma^*$ charge transfer (see below). All these three quantitative parameters are well correlated with the C≡N bond length shortening. However, the best results are obtained when this is correlated with the fundamental observation of the N lone-pair charge decrease as

TABLE 6: Modifications of the Acetonitrile C≡N Stretching Band Parameters Calculated at the B3LYP/6-31++G(2d,2p) Level of Theory

acid	*d*(C≡N) (Å)	Δ*d*(C≡N) (%)	*ν*(C≡N) (cm^{-1})	Δ*ν*(C≡N) (cm^{-1})	Δ*ν*(C≡N) (%)	IR intens (km/mol)	Raman intens (Å⁴/amu)	acid α (Å³)
BO_2H	1.1534	−0.3198	2385.5	25.3	1.0724	47.4	110.9	2.866
BO_3H_3	1.1545	−0.2247	2378.0	17.8	0.7536	26.7	109.1	3.968
CF_3COOH	1.1534	−0.3198	2385.0	24.8	1.0515	44.2	117.9	5.271
CF_3OH	1.1535	−0.3111	2384.7	24.5	1.0371	40.8	107.3	3.320
CF_3SO_3H	1.1526	−0.3889	2391.0	30.8	1.3063	53.4	122.2	7.018
CH_2NOH	1.1544	−0.2333	2378.4	18.2	0.7726	27.9	114.0	4.090
CH_3COOH	1.1546	−0.2157	2376.1	15.8	0.6714	29.1	118.4	4.910
CH_3OH	1.1553	−0.1556	2372.3	12.1	0.5107	23.4	106.9	2.915
CH_3SO_3H	1.1536	−0.3025	2383.9	23.7	1.0056	40.7	120.6	6.528
C_6H_5OH	1.1547	−0.2048	2375.3	15.1	0.6378	26.0	151.7	10.905
ClCOOH	1.1534	−0.3198	2385.6	25.4	1.0779	45.1	121.7	4.985
ClOH	1.1541	−0.2622	2380.8	20.6	0.8716	32.7	110.7	2.900
ClO_2H	1.1540	−0.2698	2381.0	20.8	0.8827	38.5	108.9	4.150
ClO_3H	1.1539	−0.2766	2381.3	21.1	0.8935	36.2	121.5	4.964
ClO_4H	1.1530	−0.3578	2388.5	28.3	1.1969	50.6	116.6	5.328
CNOH	1.1529	−0.3651	2389.2	29.0	1.2278	53.8	106.9	3.081
CO_3H_2	1.1537	−0.2938	2383.1	22.9	0.9705	36.4	110.3	3.740
FCOOH	1.1533	−0.3284	2385.9	25.7	1.0878	43.2	106.9	3.198
FOH	1.1541	−0.2635	2380.9	20.7	0.8770	34.3	101.0	1.587
H_2O	1.1555	−0.1383	2371.0	10.8	0.4590	22.8	96.4	1.205
H_2O_2	1.1546	−0.2161	2376.8	16.6	0.7023	26.7	102.6	2.059
HCOOH	1.1542	−0.2506	2379.7	19.5	0.8267	34.9	108.2	3.178
NH_2OH	1.1549	−0.1864	2374.9	14.6	0.6205	22.6	104.6	2.541
NO_2H	1.1541	−0.2558	2380.0	19.7	0.8364	35.8	114.1	3.003
NO_3H	1.1534	−0.3198	2385.2	24.9	1.0570	42.8	118.3	3.716
SO_3H_2	1.1540	−0.2677	2380.8	20.6	0.8732	34.8	115.1	5.165
SO_4H_2	1.1531	−0.3457	2387.6	27.4	1.1612	47.4	114.4	5.286
CH_3CN	***1.1571***		***2360.2***			***11.8***	***74.13***	

TABLE 7: Natural Bond Order Analysis Results for the C≡N Bond in HB Complexes at the B3LYP/6-31++G(2d,2p) Level of Theory (LP = Lone Pair; *e* = Electrons; *me* = Millielectrons)

acid	ρ(N) LP (*e*)	$\Delta\rho$(N) LP (*me*)	ρ (*e*)	ρ^* (*e*)	$\Delta\rho$ (*me*)	B → A charge transfer (*me*)	% natural hybrid *s* character C	% natural hybrid *s* character N	C≡N Δ s character
BO_2H	1.9178	−47.34	5.9762	0.0886	−9.85	51.68	48.67	46.28	2.20
BO_3H_3	1.9421	−23.10	5.9749	0.0831	−5.69	25.38	47.52	46.68	1.45
CF_3COOH	1.9170	−48.20	5.9756	0.0882	−10.11	51.85	48.48	46.36	2.09
CF_3OH	1.9206	−44.56	5.9758	0.0873	−9.04	48.19	48.46	46.38	2.09
CF_3SO_3H	1.8988	−66.37	5.9757	0.0906	−12.44	71.06	49.08	46.18	2.51
CH_2NOH	1.9393	−25.84	5.9750	0.0837	−6.25	27.70	47.61	46.66	1.52
CH_3COOH	1.9377	−27.49	5.9755	0.0863	−8.39	29.54	47.73	46.58	1.56
CH_3OH	1.9498	−15.38	5.9749	0.0825	−5.06	16.75	47.08	46.80	1.13
CH_3SO_3H	1.9186	−46.53	5.9750	0.0882	−10.64	48.92	48.22	46.46	1.93
C_6H_5OH	1.9423	−22.87	5.9751	0.0844	−6.79	25.19	47.53	46.66	1.44
ClCOOH	1.9150	−50.15	5.9756	0.0884	−10.36	53.45	48.51	46.36	2.12
ClOH	1.9313	−33.87	5.9755	0.0859	−7.88	34.55	47.96	46.55	1.76
ClO_2H	1.9269	−38.30	5.9755	0.0877	−9.77	39.58	48.09	46.49	1.83
ClO_3H	1.9266	−38.56	5.9755	0.0874	−9.35	41.01	48.16	46.46	1.87
ClO_4H	1.9065	−58.69	5.9760	0.0900	−11.54	61.70	48.88	46.25	2.38
CNOH	1.9045	−60.71	5.9763	0.0906	−11.78	65.47	49.05	46.17	2.47
CO_3H_2	1.9257	−39.48	5.9750	0.0864	−8.94	42.19	48.06	46.52	1.83
FCOOH	1.9163	−48.91	5.9756	0.0883	−10.23	52.56	48.50	46.37	2.12
FOH	1.9295	−35.65	5.9756	0.0864	−8.25	36.21	48.05	46.51	1.81
H_2O	1.9526	−12.61	5.9751	0.0821	−4.48	13.65	47.09	46.78	1.12
H_2O_2	1.9410	−24.17	5.9752	0.0840	−6.27	24.43	47.51	46.69	1.45
HCOOH	1.9297	−35.43	5.9747	0.0866	−9.43	37.27	47.74	46.60	1.59
NH_2OH	1.9459	−19.28	5.9748	0.0824	−5.14	19.50	47.22	46.78	1.25
NO_2H	1.9310	−34.16	5.9756	0.0860	−7.86	37.01	48.04	46.51	1.80
NO_3H	1.9174	−47.80	5.9756	0.0882	−10.12	49.82	48.49	46.38	2.12
SO_3H_2	1.9271	−38.12	5.9754	0.0864	−8.48	40.02	48.05	46.50	1.80
SO_4H_2	1.9094	−55.78	5.9754	0.0893	−11.43	59.35	48.63	46.33	2.21
CH_3CN	***1.9652***		***5.9741***	***0.0766***			***45.54***	***47.21***	

can be observed in Figure 4, which shows the absolute values of both parameters. The fitting obeys the following power (multiplicative) function:

$$|\Delta d(\mathrm{C{\equiv}N})| = 1.9577 \pm 0.1048|\Delta\rho|^{0.6718\ \pm 0.0155}$$

$$r = -0.9917, \quad R^2 = 98.35\%, \quad N = 27,$$
$$\text{standard error of the estimate} = 0.0334$$

It is interesting to assess the consequences of the HB formation on the O−H bond population. As can be observed in Table 8, there is a general and significant increase in the antibonding electron population which is further accompanied by a slight decrease in the corresponding bonding population. It is noteworthy that the reported increase in the antibonding population almost exactly coincides with the net charge transfer (see Table 7) which justifies the n → σ^* mechanism proposed[65,67,68,70] for HB formation. These results will be correlated in the next section of this paper with the calculated O−H bond elongation.

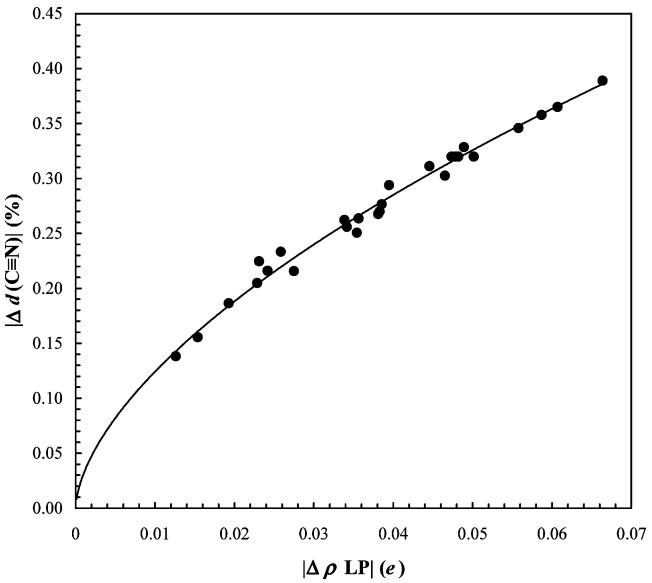

Figure 4. Relative % change (absolute values) of the C≡N bond length against relative decrease in the total ($\sigma + \pi' + \pi''$) antibonding population in the triple bond after HB formation.

As a consequence of the C≡N bond shortening, its stretching frequency shifts toward higher wavenumbers. These shifts are significant (from 10.8 cm^{-1} in the H_2O complex up to 30.8 cm^{-1} in the CF_3SO_3H complex) and imply the presence of a discrete new band in the vibrational spectra. Surprisingly, there is not in the literature, to the best of our knowledge, a great deal of information about vibrational studies of H-bound acetonitrile complexes in the gas phase that should allow the experimental comparison with the calculated values presented here. Coussan et al.[10] report a shift of 9.3 cm^{-1} (calculated: 12.1 cm^{-1}) in acetonitrile−methanol complexes while Kryachko and the Nguyen[13] quote a value of 12.5 cm^{-1} (calculated: 15.1 cm^{-1}) in phenol−acetonitrile complexes. In other types of complex, the H-bonding of acetonitrile to hydrogen fluoride[71] promotes a shift of 32 cm^{-1} in the C≡N stretching band that we have evaluated in 27 cm^{-1} at the same level of theory used in the present work. Therefore, we can conclude that the experimental results are, probably, fairly well reproduced in our computational approach.

Figure 5 illustrates the relationship between the shortening of the C≡N bond and the geometry (N···H length) of the HB. The fitted line corresponds to an inverse of the X function with the following results:

$$d(\mathrm{C} \equiv \mathrm{N}) = 1.1685 \pm 0.0004 - \frac{0.0269 \pm 0.0007}{d(\mathrm{N} \cdots \mathrm{H})}$$

$$r = -0.9912, \quad R^2 = 98.26\%,$$
$$\text{standard error of the estimate} = < 0.0001$$

TABLE 8: Natural Bond Order Analysis Results for the O−H Bond in HB Complexes at the B3LYP/6-31++G(2d,2p) Level of Theory (*e* = Electrons; *me* = Millielectrons)

	acid		complex				
acid	ρ (*e*)	ρ^* (*e*)	ρ (*e*)	ρ^* (*e*)	$\Delta\rho$ (*me*)	$\Delta\rho^*$ (*me*)	total Δ (*me*)
BO_2H	1.976 80	0.004 72	1.974 03	0.056 23	−2.77	51.51	54.28
BO_3H_3	1.985 04	0.005 65	1.984 54	0.032 17	−0.50	26.52	27.02
CF_3COOH	1.984 60	0.012 79	1.982 91	0.065 83	−1.69	53.04	54.73
CF_3OH	1.975 29	0.006 27	1.971 80	0.055 87	−3.49	49.60	53.09
CF_3SO_3H	1.986 14	0.006 61	1.983 46	0.078 56	−2.68	71.95	74.63
CH_2NOH	1.992 29	0.003 24	1.991 51	0.032 68	−0.78	29.44	30.22
CH_3COOH	1.985 54	0.008 07	1.984 37	0.038 77	−1.17	30.70	31.87
CH_3OH	1.991 13	0.005 57	1.990 37	0.023 10	−0.76	17.53	18.29
CH_3SO_3H	1.987 81	0.006 19	1.985 08	0.058 12	−2.73	51.93	54.66
C_6H_5OH	1.987 33	0.007 18	1.987 12	0.033 00	−0.21	25.82	26.03
ClCOOH	1.978 37	0.012 81	1.974 19	0.067 07	−4.18	54.26	58.44
ClOH	1.997 04	0.002 41	1.995 44	0.039 80	−1.60	37.39	38.99
ClO_2H	1.997 06	0.005 07	1.996 19	0.047 79	−0.87	42.72	43.59
ClO_3H	1.992 76	0.007 82	1.988 72	0.049 78	−4.04	41.96	46.00
ClO_4H	1.988 35	0.005 96	1.984 98	0.070 42	−3.37	64.46	67.83
CNOH	1.968 62	0.009 29	1.963 79	0.073 35	−4.83	64.06	68.89
CO_3H_2	1.982 33	0.006 17	1.980 16	0.050 91	−2.17	44.74	46.91
FCOOH	1.979 67	0.006 85	1.976 43	0.061 09	−3.24	54.24	57.48
FOH	1.996 62	0.002 51	1.995 75	0.042 16	−0.87	39.65	40.52
H_2O	1.999 47	0.000 01	1.998 03	0.015 64	−1.44	15.63	17.07
H_2O_2	1.996 19	0.003 80	1.995 45	0.030 88	−0.74	27.08	27.82
HCOOH	1.988 13	0.015 75	1.986 85	0.055 52	−1.28	39.77	41.05
NH_2OH	1.994 55	0.004 19	1.993 57	0.025 72	−0.98	21.53	22.51
NO_2H	1.990 68	0.007 55	1.988 89	0.047 14	−1.79	39.59	41.38
NO_3H	1.988 22	0.010 07	1.985 90	0.063 44	−2.32	53.37	55.69
SO_3H_2	1.992 75	0.014 54	1.992 41	0.057 91	−0.34	43.37	43.71
SO_4H_2	1.986 20	0.006 69	1.983 38	0.067 74	−2.82	61.05	63.87

Attempts to fit the dependent variable with other parameters (ΔE, EPH) give significantly worse results. However, the fitting of d(C≡N) against ΔE, although statistically less significant ($r = -0.9732$), predicts a value of 1.1580 ± 0.0002 Å (experimental: 1.1571 Å) for d(C≡N) at $\Delta E = 0$.

The C≡N stretching frequency shifts against the C≡N bond length are plotted in Figure 6. As could be expected, the best function which describes the dependence between both variables is linear:

$$\Delta\nu(\mathrm{C}\equiv\mathrm{N}) = 8185 \pm 117 - (7075 \pm 102)d(\mathrm{C}\equiv\mathrm{N})$$

$$r = -0.9974, \quad R^2 = 99.49\%,$$
$$\text{standard error of the estimate} = 0.3768$$

The C≡N stretching shift that should correspond to a bond length of 1.1571 Å (experimental bond length in gaseous acetonitrile) is -1.0 ± 1.0 cm^{-1}, which offers an acceptable level of self-consistency in the data.

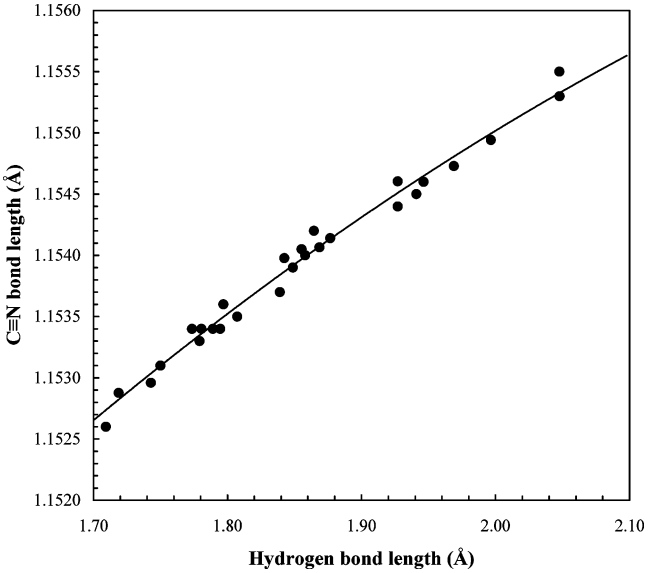

Figure 5. Relationship between the C≡N bond length in the complexes and the geometry (N···H length) of the HB.

Infrared and Raman intensities are, as can be observed in Table 9, strongly affected by the HB formation. In both cases, there is a considerable increase of the spectral band intensity, as could be expected from previous experimental[4,9,10] and computational[4,5,13,14] results. To clarify the calculated results, a systematic study of the statistical dependence of both Raman and Infrared band intensities was carried out. The situation with the IR intensity seems to be quite simple: as can be observed in Figure 7, absolute IR intensities depend on the energy of the hydrogen bond in a linear way. The fitted equation is

$$I_{\mathrm{IR}} = 9.1790 \pm 0.8298 + (0.9960 \pm 0.0283)|\Delta E|$$

$$r = -0.9900, \quad R^2 = 98.03\%,$$
$$\text{standard error of the estimate} = 1.3428$$

Taking into account the IR intensity in CH_3CN (11.8 km/mol), which corresponds in the fitted equation with $|\Delta E| = 0$, the relative error is not too high and the results obtained in the HB complexes predict fairly well the calculated value for the base. However, the situation is much more complex in the case of the Raman intensities. None of the studied parameters can justify, by itself, the calculated increases. So, as the influence could be multifactorial, a multiple regression procedure was undertaken. As initial variables, ΔE, d(N···H), d(C≡N), $\Delta\nu$(C≡N), IR intensity and polarizability and EPH of the acid were considered. The final model selected, which does not contain any constant element, resulted in the following:

$$I_{\mathrm{Raman}} = (0.7305 \pm 0.0530)\alpha + (80.4217 \pm 1.4136)d(\mathrm{C}\equiv\mathrm{N})$$

$$R^2 = 99.91\%, \quad \text{standard error of the estimate} = 3.5531$$

Table 9 gives computational and fitted results. As can be observed, all but two percent errors are lower than ±5%. Thus,

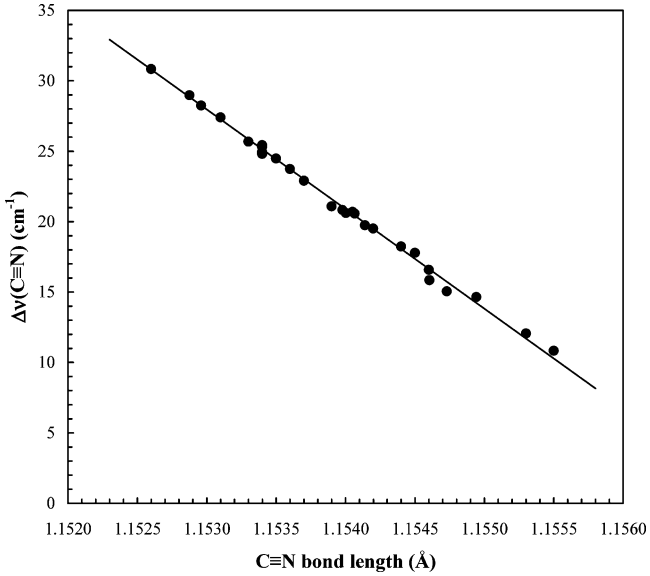

Figure 6. C≡N stretching frequency shifts [$\nu(C{\equiv}N)_{complex} - \nu(C{\equiv}N)_{CH_3CN}$] against complex C≡N bond length.

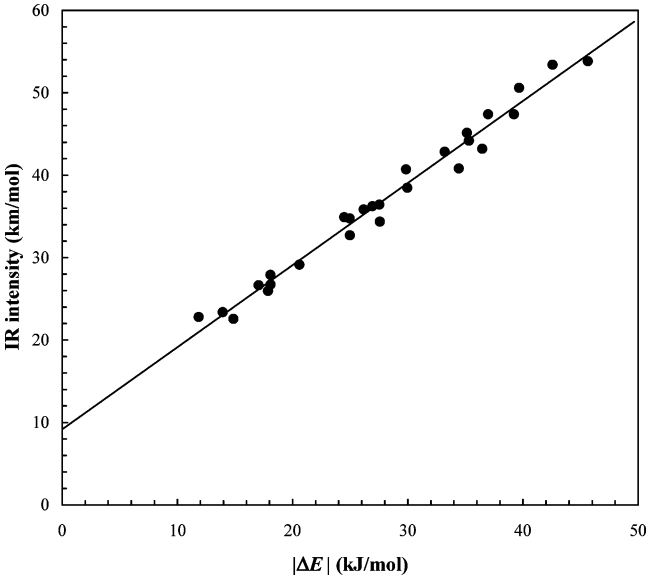

Figure 7. C≡N stretching IR intensities against the absolute values of BSSE corrected ΔE.

TABLE 9: Calculated and Fitted Raman Intensities (Å⁴/amu)

acid	calculated intensity	fitted intensity	error %
BO_2H	110.9	106.9	3.61
BO_3H_3	109.1	112.4	−2.99
CF_3COOH	117.9	118.7	−0.70
CF_3OH	107.3	109.1	−1.74
CF_3SO_3H	122.2	127.3	−4.16
CH_2NOH	114.0	113.0	0.90
CH_3COOH	118.4	117.1	1.16
CH_3OH	106.9	107.3	−0.35
CH_3SO_3H	120.6	125.0	−3.62
C_6H_5OH	151.7	146.6	3.36
ClCOOH	121.7	117.3	3.60
ClOH	110.7	107.1	3.26
ClO_2H	108.9	113.3	−4.05
ClO_3H	121.5	117.3	3.44
ClO_4H	116.6	119.0	−2.03
CNOH	106.9	107.9	−0.98
CO_3H_2	110.3	111.2	−0.83
FCOOH	106.9	108.5	−1.55
FOH	101.0	100.6	0.33
H_2O	96.4	98.9	−2.59
H_2O_2	102.6	103.0	−0.45
HCOOH	108.2	108.5	−0.30
NH_2OH	104.6	105.4	−0.73
NO_2H	114.1	107.6	5.70
NO_3H	118.3	111.1	6.13
SO_3H_2	115.1	118.3	−2.76
SO_4H_2	114.4	118.8	−3.82

the increase in the Raman intensity after HB formation seems to depend on one property of the H-donating acid, its polarizability, and another which is characteristic of the HB complex itself, i.e.: the bound-acetonitrile C≡N bond length. Furthermore, this parameter directly depends, as we have previously discussed, on the geometrical factors of the hydrogen bond.

3.4. Vibrational Changes in the O—H Stretch. Even though the main objective of the present work is to study in detail the HB effects on the nitrile C≡N bond vibrational dynamics, the O−H bond characteristics are obviously related. Table 10 summarizes the O−H geometric and vibrational modifications calculated for the acids considered here. In total agreement with previous theoretical and experimental results,[45,48,50,72−75] there is a considerable elongation of the bond which results from the HB formation. This elongation, which likewise justifies the observed downshift of the O−H stretching wavenumbers, can be correlated with the HB length (see Figure 8) and hence with the occupancy increase of the O−H antibonding orbital, as can be observed in Figure 9 which represents the proportional (%) elongation of the O−H bond against the total Δ parameter computed as

$$\text{total } \Delta = \Delta\rho^* - \Delta\rho$$

for the corresponding σ orbital. The fitting obeys again a power (multiplicative) function with the following parameters:

$$\Delta d(\text{O}-\text{H}) = (0.0304 \pm 0.0038)(\text{total } \Delta)^{1.0717\pm0.0313}$$

$$r = -0.9895, \quad R^2 = 97.91\%, \quad N = 27,$$
$$\text{standard error of the estimate} = 0.0643$$

Thus, the charge-transfer process, which is the *ultima ratio* of the hydrogen bond formation, seems to account for the main vibrational changes observed both in the donor and in the acceptor molecules.

4. Conclusions

(1) Observed nitrile C≡N bond shortening and the consequent vibrational stretching blue-shift promoted by HB formation have been reasonably well reproduced using density functional theory-based calculations.

(2) For the first time, C≡N bond shortening has been accounted for by three different, although interconnected, reasons mostly promoted by the charge-transfer process: important depletion in the electronic population of the N lone pair; relative decrease in the total ($\sigma + \pi' + \pi''$) antibonding population; and significant increase in the *s* character of the triple bond.

(3) Observed increases in the C≡N stretching IR and Raman band intensities can be explained by the intensity of the HB interaction (IR intensity) and by a combination of this parameter *plus* the mean polarizability of the donor acid (Raman intensity).

(4) O−H bond elongation can be regarded as another consequence of the charge transfer process as far as the HB formation means fundamentally that a significant part of the lone pair electrons are transferred into the O−H antibonding σ

TABLE 10: Modifications of the O−H Stretching Band Parameters Calculated at the B3LYP/6-31++G(2d,2p) Level of Theory[a]

acid	acid *d* OH (Å)	complex *d* OH (Å)	acid ν OH (cm^{-1})	complex ν OH (cm^{-1})	$\Delta\nu$ OH (cm^{-1})	IR intensity ratio	Raman intensity ratio
BO_2H	0.9621	0.9858	3878.9	3390.6	−488.4	11.30	4.20
BO_3H_3	0.9619	0.9729	3872.6	3647.3	−225.3	10.18	5.66
CF_3COOH	0.9705	0.9922	3752.6	3316.2	−436.4	17.86	3.60
CF_3OH	0.9661	0.9863	3817.6	3410.9	−406.7	15.51	4.07
CF_3SO_3H	0.9706	1.0025	3763.1	3127.4	−635.7	16.66	4.51
CH_2NOH	0.9639	0.9751	3832.4	3616.7	−215.7	11.98	4.15
CH_3COOH	0.9651	0.9767	3811.1	3585.3	−225.8	19.76	3.75
CH_3OH	0.9618	0.9682	3848.4	3732.8	−115.6	17.67	3.05
CH_3SO_3H	0.9688	0.9903	3785.2	3348.3	−436.9	13.53	4.70
C_6H_5OH	0.9632	0.9729	3833.8	3643.7	−190.1	16.24	3.67
ClCOOH	0.9712	0.9937	3742.6	3294.8	−447.7	20.49	3.78
ClOH	0.9688	0.9831	3781.5	3504.6	−276.9	13.81	4.03
ClO_2H	0.9716	0.9880	3742.7	3420.9	−321.9	15.24	3.34
ClO_3H	0.9738	0.9909	3724.4	3382.9	−341.5	14.06	5.24
ClO_4H	0.9741	1.0020	3721.3	3173.6	−547.7	16.65	4.18
CNOH	0.9683	0.9970	3774.4	3206.6	−567.8	14.69	3.43
CO_3H_2	0.9669	0.9849	3807.3	3443.9	−363.4	7.27	2.63
FCOOH	0.9684	0.9907	3790.2	3338.8	−451.5	14.89	4.51
FOH	0.9722	0.9864	3744.6	3472.7	−271.8	20.82	3.76
H_2O	0.9626	0.9700	3815.6	3718.0	−97.6	7.17	6.37
H_2O_2	0.9679	0.9773	3777.4	3606.1	−171.3	12.37	6.69
HCOOH	0.9713	0.9867	3737.6	3429.8	−307.9	18.01	3.81
NH_2OH	0.9632	0.9710	3827.7	3689.3	−138.4	14.37	3.63
NO_2H	0.9699	0.9849	3766.4	3474.5	−291.9	15.82	3.58
NO_3H	0.9727	0.9948	3731.0	3303.1	−427.9	15.85	4.98
SO_3H_2	0.9726	0.9894	3722.5	3386.3	−336.2	12.95	2.55
SO_4H_2	0.9696	0.9962	3775.6	3242.7	−533.0	38.50	2.71

[a] Intensity ratios are $I_{complex}/I_{acid}$.

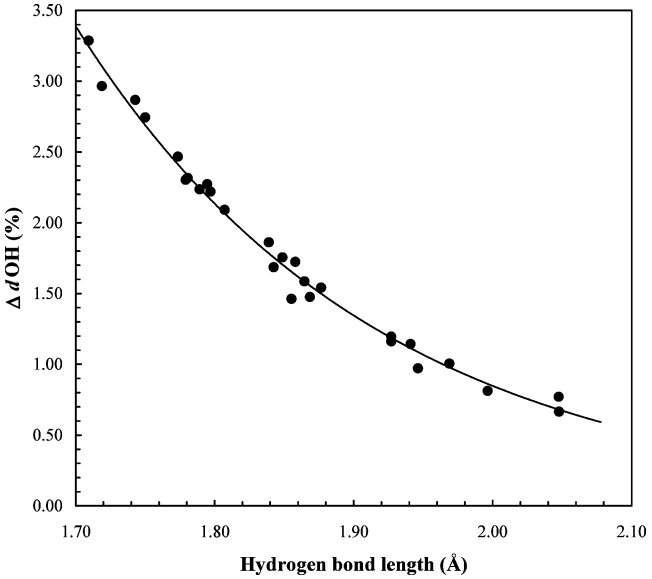

Figure 8. Relative (%) elongation of the O−H bond against the HB length.

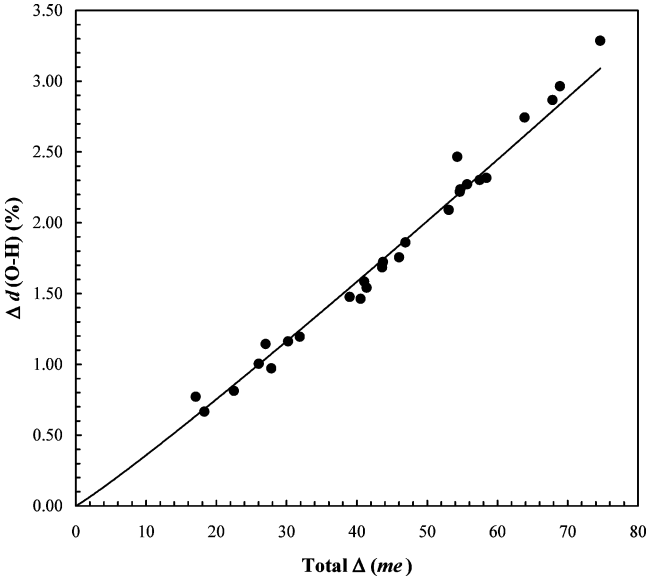

Figure 9. Relative (%) elongation of the O−H bond in the complexes as a function of the antibonding σ orbital population increase.

orbital. In fact, nearly all the charge transferred arises from the N lone pair and seems to go directly to this antibonding orbital, thus justifying the HB formation as a n → σ* process.

(5) This systematic computational work further demonstrates that, even in relatively complex systems, the HB main energetic, geometric and vibrational characteristics can be predicted using density functional theory with an acceptable level of confidence.

Acknowledgment. The technical support of Javier Ayllon, from Castilla-La Mancha University Supercomputation Center, is gratefully recognized.

References and Notes

(1) Sadlej, J. *Spectrochim. Acta A* **1979**, *35*, 681.
(2) Dimitrova, Y. *J. Mol. Struct. (THEOCHEM)* **1995**, *334*, 215.
(3) Dimitrova, Y. *J. Mol. Struct. (THEOCHEM)* **1995**, *343*, 25.
(4) Moliner, A. K.; Brooksby, P. A.; Loring, J. S.; Bako, I.; Pálinkás, G.; Fawcett, W. R. *J. Phys. Chem. A* **2004**, *108*, 3344.
(5) Pejov, L. *Int. J. Quantum Chem.* **2002**, *86*, 356.
(6) Hirao, K.; Yamabe, S.; Sano, M. *J. Phys. Chem.* **1982**, *86*, 2626.
(7) Perelygin, I. S. In *Ionic Solvation*; Krestov, G. A., et al., Eds.; Ellis Horwood: Chichester, U.K., 1994; p 100.
(8) Alía, J. M. in *Handbook of Raman Spectroscopy. From the Research Laboratory to the Process Line*, 1st ed.; Lewis, I. R., Edwards, H. G. M., Eds.; Marcel Dekker: New York, 2001; p 617.

(9) Vijay, A.; Sathyanarayana, D. N. *J. Phys. Chem.* **1996**, *100*, 75.
(10) Coussan, S.; Bouteiller, Y.; Perchard, J. P.; Brenner, V.; Millié, P.; Zheng, W. Q.; Talbot, F. *J. Chem. Phys.* **1999**, *110*, 10046.
(11) Galabov, B.; Bobadova-Parvanova, P. *J. Phys. Chem. A* **1999**, *103*, 6793.
(12) George, W. O.; Jones, B. F.; Lewis, R.; Price, J. M. *Phys. Chem. Chem. Phys.* **2000**, *2*, 4910.
(13) Kryachko, E. S.; Nguyen, M. T. *J. Phys. Chem. A* **2002**, *106*, 4267.
(14) Rissi, E.; Fileti, E. E.; Canuto, S. *Theor. Chem. Acc.* **2003**, *110*, 360.
(15) Chaban, G. M. *J. Phys. Chem. A* **2004**, *108*, 4551.
(16) Pemberton, R. S.; Shurvell, H. F. *J. Raman Spectrosc.* **1995**, *26*, 373.
(17) Girling, R. B.; Shurvell, H. F. *Vibr. Spectrosc.* **1998**, *18*, 77.
(18) Quadri, S. M.; Shurvell, H. F. *Spectrochim. Acta A* **1995**, *51*, 1355.
(19) Singh, R. K.; Asthana, B. P.; Singh, P. R.; Chakraborty, T.; Verma, A. L. *J. Raman Spectrosc.* **1998**, *29*, 561.
(20) Alía, J. M.; Edwards, H. G. M.; Kiernan, B. M. *Spectrochim. Acta A* 2004, in press.
(21) Nakabayashi, T.; Nishi, N. *J. Phys. Chem. A* **2002**, *106*, 3491.
(22) Del Bene, J. E.; Person, W. B.; Szczepaniak, K. *J. Phys. Chem.* **1995**, *99*, 10705.
(23) Novoa, J. J.; Sosa, C. *J. Phys. Chem.* **1995**, *99*, 15837.
(24) Pudzianowski, A. T. *J. Phys. Chem.* **1996**, *100*, 4781.
(25) Dimitrova, Y. *Spectrochim. Acta A* **2004**, *60*, 1.
(26) Schlücker, S.; Singh, R. K.; Asthana, B. P.; Popp, J.; Kiefer, W. *J. Phys. Chem. A* **2001**, *105*, 9983.
(27) . Burneau, A.; Génin, F.; Quilés, F. *Phys. Chem. Chem. Phys.* **2000**, *2*, 5020.
(28) Ireta, J.; Neugebauer, J.; Scheffler, M. *J. Phys. Chem. A* **2004**, *108*, 5692.
(29) Lide, D. R. *Handbook of Chemistry and Physics*; CRC Press: Boca Raton, FL, 1993.
(30) Harmony, M. D.; Laurie, V. W.; Kuczkowski, R. L.; Schwendeman, R. H.; Ramsay, D. A.; Lovas, F. J.; Lafferty, W. J.; Maki, A. G. *J. Phys. Chem. Ref. Data* **1979**, *8*, 619.
(31) Becke, A. D. *Phys. Rev. A* **1988**, *37*, 3098.
(32) Lee, C.; Yang, W.; Parr, R. G. *Phys. Rev. B* **1988**, *37*, 785.
(33) Becke, A. D. *J. Chem. Phys.* **1993**, *98*, 5648.
(34) Simon, S.; Duran, M.; Dannemberg, J. J. *J. Chem. Phys.* **1996**, *105*, 11024.
(35) Boys, S. F.; Bernardi, F. *Mol. Phys.* **1970**, *19*, 553.
(36) Gaussian 03, Revision B.03, Frisch, M. J.; Trucks, G. W.; Schlegel, H. B.; Scuseria, G. E.; Robb, M. A.; Cheeseman, J. R.; Montgomery, Jr. J. A.; Vreven, T.; Kudin, K. N.; Burant, J. C.; Millam, J. M.; Iyengar, S. S.; Tomasi, J.; Barone, V.; Mennucci, B.; Cossi, M.; Scalmani, G.; Rega, N.; Petersson, G. A.; Nakatsuji, H.; Hada, M.; Ehara, M.; Toyota, K.; Fukuda, R.; Hasegawa, J.; Ishida, M.; Nakajima, T.; Honda, Y.; Kitao, O.; Nakai, H.; Klene, M.; Li, X.; Knox, J. E.; Hratchian, H. P.; Cross, J. B.; Adamo, C.; Jaramillo, J.; Gomperts, R.; Stratmann, R. E.; Yazyev, O.; Austin, A. J.; Cammi, R.; Pomelli, C.; Ochterski, J. W.; Ayala, P. Y.; Morokuma, K.; Voth, G. A.; Salvador, P.; Dannenberg, J. J.; Zakrzewski, V. G.; Dapprich, S.; Daniels, A. D.; Strain, M. C.; Farkas, O.; Malick, D. K.; Rabuck, A. D.; Raghavachari, K.; Foresman, J. B.; Ortiz, J. V.; Cui, Q.; Baboul, A. G.; Clifford, Cioslowski, J. I.; Stefanov, B. B.; Liu, G.; Liashenko, A.; Piskorz, P.; Komaromi, I.; Martin, R. L.; Fox, D. J.; Keith, T.; Al-Laham, M. A.; Peng, C. Y.; Nanayakkara, A.; Challacombe, M.; Gill, P. M. W.; Johnson, B.; Chen, W.; Wong, M. W.; Gonzalez, C. Pople, J. A. Gaussian, Inc.: Pittsburgh, PA, 2003. Institutional License, UCLM.
(37) Semichem Inc., PO Box 1649, Shawnee Mission, KS, Institutional License, UCLM.
(38) Statistical Graphics Corp., Institutional License, UCLM.
(39) Koga, Y.; Kondo, S.; Saeki, S. *J. Phys. Chem.* **1984**, *88*, 3152.
(40) Shimanouchi, T. *J. Phys. Chem. Ref. Data* **1977**, *6*, 993.
(41) Fuson, N.; Josien, M.-L.; Jones, E. A.; Lawson, J. R. *J. Chem. Phys.* **1952**, *20*, 1627.
(42) Barceló, J. R.; Otero, C. *Spectrochim. Acta* **1962**, *18*, 1231.
(43) Durig, J. R.; Zhou, L.; Schwartz, T.; Gounev, T. *J. Raman Spectrosc.* **2000**, *31*, 193.
(44) Andersson, M. P.; Uvdal, P. *J. Phys. Chem. A* **2005**, *109*, 2937.
(45) Gilli, G.; Gilli, P. *J. Mol. Struct.* **2000**, *552*, 1.
(46) Le Questel, J.-Y.; Berthelot, M.; Laurence, C. *J. Phys. Org. Chem.* **2000**, *13*, 347.
(47) Grabowski, S. J. *J. Phys. Chem. A* **2001**, *105*, 10739.
(48) Sokolov, N. D. *Ann. Chim. (Paris)* **1965**, *10*, 497.
(49) Lindgren, J.; Tegenfeldt, J. *J. Mol. Struct.* **1974**, *20*, 335.
(50) Sokolov, N. D. *J. Mol. Struct.* **1997**, *436*−*437*, 201.
(51) Meot-Ner (Mautner), M. *Chem. Rev.* **2005**, *105*, 213.
(52) Bondi, A. *J. Phys. Chem.* **1964**, *68*, 441.
(53) Dimitrova, V.; Ilieva, S.; Galabov, B. *J. Phys. Chem. A* **2002**, *106*, 11801.
(54) Galabov, B.; Bobadova-Parvanova, P.; Ilieva, S.; Dimitrova, V. *J. Mol. Struct. (THEOCHEM)* **2003**, *630*, 101.
(55) Dimitrova, V.; Ilieva, S.; Galabov, B. *J. Mol. Struct. (THEOCHEM)* **2003**, *637*, 73.
(56) Galabov, B.; Cheshmedzhieva, D.; Ilieva, S.; Hadjieva, B. *J. Phys. Chem. A* **2004**, *108*, 11457.
(57) Alía, J. M.; Edwards, H. G. M.; Moore, J. *Spectrochim. Acta A* **1996**, *52*, 1403.
(58) Alía, J. M.; Edwards, H. G. M. *J. Mol. Struct.* **1995**, *354*, 97.
(59) Hunter, E. P. L.; Lias, S. G. *J. Phys. Chem. Ref. Data* **1998**, *27*, 413.
(60) Zhou, Z.; Shi, Y.; Zhou, X. *J. Phys. Chem. A* **2004**, *108*, 813.
(61) Max, J.-J.; Chapados, C. *J. Chem. Phys.* **2005**, *112*, 014504−1.
(62) Max, J.-J.; Chapados, C. *J. Chem. Phys.* **2003**, *119*, 5632.
(63) Alía, J. M.; Edwards, H. G. M.; García, F. J. *J. Mol. Struct.* **1999**, *508*, 51.
(64) Marcos, C.; Alía, J. M.; Adovasio, V.; Prieto, M.; García Granda, S. *Acta Crystallogr. C* **1998**, *54*, 1225.
(65) Hobza, P.; Havlas, Z. *Chem. Rev.* **2000**, *100*, 4253.
(66) NBO Version 3.1, Glendening, E. D.; Reed, A. E.; Carpenter, J. E.; Weinhold, F.
(67) Foster, J. P.; Weinhold, F. *J. Am. Chem. Soc.* **1980**, *102*, 7211.
(68) Reed, A. E.; Curtiss, L. A.; Weinhold, F. *Chem. Rev.* **1988**, *88*, 899.
(69) Bent, H. A. *Chem. Rev.* **1961**, *61*, 275.
(70) Koch, U.; Popelier, P. L. A. *J. Phys. Chem.* **1995**, *99*, 9747.
(71) Johnson, G. L.; Andrews, L. *J. Phys. Chem.* **1983**, *87*, 1852.
(72) Efimov, Y. Ya.; Naberukin, Y. I. *Mol. Phys.* **1975**, *30*, 1621.
(73) Efimov, Y. Ya.; Naberukin, Y. I. *Mol. Phys.* **1975**, *30*, 1635.
(74) Efimov, Y. Ya.; Naberukin, Y. I. *Faraday Discuss. Chem. Soc.* **1988**, *85*, 117.
(75) Bricknell, B. C.; Ford, T. A.; Letcher, T. M. *Spectrochim. Acta A* **1997**, *53*, 299.